SUPPORTING INFORMATION

A highly orientational architecture formed by covalently bonded graphene for achieving high through-plane thermal conductivity of polymer composites

Qingwei Yan,[a,b,c,#] Jingyao Gao,[d,#] Ding Chen,[e,*] Peidi Tao,[b] Lu Chen,[b,c] Junfeng Ying,[b,c] Xue Tan,[b,c] Le Lv,[b,c] Wen Dai,[b,c] Fakhr E. Alam,[f,*] Jinhong Yu,[b,c] Yuezhong Wang,[b,c] He Li,[b,c] Chen Xue,[b,c] Kazuhito Nishimura,[g] Sudong Wu,[h,i,*] Nan Jiang,[b,c] and Cheng-Te Lin[a,b,c,*]

[a] *Qianwan Institute, Ningbo Institute of Materials Technology and Engineering (NIMTE), Chinese Academy of Sciences, Ningbo 315201, P.R. China.*

[b] *Key Laboratory of Marine Materials and Related Technologies, Zhejiang Key Laboratory of Marine Materials and Protective Technologies, Ningbo Institute of Materials Technology and Engineering (NIMTE), Chinese Academy of Sciences, Ningbo 315201, P.R. China.*

[c] *Center of Materials Science and Optoelectronics Engineering, University of Chinese Academy of Sciences, Beijing 100049, P.R. China.*

[d] *Jiangxi Copper Technology Research Institute Co., Ltd*

[e] *State Key Laboratory of Advanced Design and Manufacturing for Vehicle Body, College of Mechanical and Vehicle Engineering, Hunan University, Changsha, 410082, P. R. China*

[f] *Department of Engineering, Applied Science Section, University of Technology and Applied Science, Nizwa Sultanate of Oman*

[g] *Advanced Nano-processing Engineering Lab, Mechanical Systems Engineering, Kogakuin University, Tokyo 192-0015, Japan.*

[h] *Academy for Advanced Interdisciplinary Studies, Southern University of Science and Technology, Shenzhen, 518055, P. R. China*

[i] *Guangdong-Hong Kong-Macao Joint Laboratory for Photonic-Thermal-Electrical Energy Materials and Devices, Southern University of Science and Technology, Shenzhen 518055, P.R. China*

[#] *Qingwei Yan and Jingyao Gao contributed equally to this work.*

** Corresponding authors*

Ding Chen: chending@hnu.edu.cn; Fakhr E. Alam: fakhr.alam@nct.edu.om; Sudong Wu: wusd@sustech.edu.cn; Cheng-Te Lin: linzhengde@nimte.ac.cn

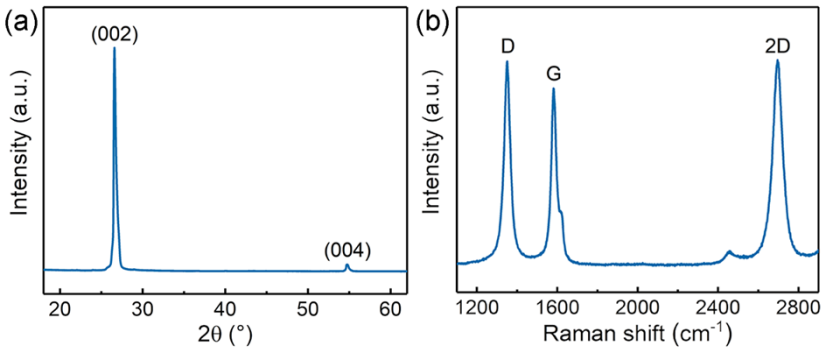

Fig. S1 (a) XRD pattern and (b) Raman spectrum of as-grown GNW.

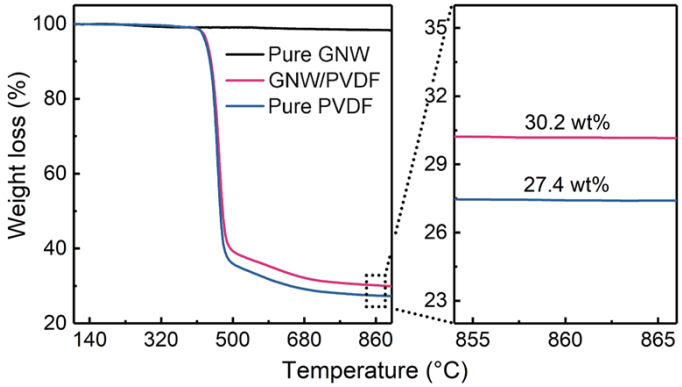

Fig. S2 TGA analysis of GNW, PVDF as well as GNW/PVDF composite, and the calculated process to determine the graphene content in the composite as shown below.

It is worth to note that the content of GNW in polymer matrix is not simply equal to the weight loss difference between the pure PVDF and GNW/PVDF composite, due to the incomplete decomposition of PVDF (with a residual weight of 27.4 wt%) and the tiny weight loss of GNW (1.6 wt%) during the heating process under nitrogen environment. Note that the GNW/PVDF composite is composed by PVDF and GNW, namely:

$$m_{PVDF} + m_{GNW} = m_{GNW/PVDF} \qquad \text{(S1)}$$

Where the $m_{GNW/PVDF}$ is the mass of GNW/PVDF, and the m_{PVDF} as well as the m_{GNW} are that of PVDF and GNW in the composite, respectively.

The residual fraction of GNW/PVDF composite (30.2 wt%) includes two parts: the GNW owning

a tiny weight loss and residual PVDF, which can be written as following equation:

$$0.274m_{PVDF} + 0.984m_{GNW} = 0.302m_{GNW/PVDF} \qquad \text{(S2)}$$

Thus, combining the equations S1 and S2, the content of GNW in the GNW/PVDF composite is determined to be 4.0 wt%.

Table S1. Comparison of the thermal conductivity enhancement (TCE) per 1 wt% graphene loading between our GNW/PVDF with other composites embedded with different graphene architectures.

Polymer matrix	TC of matrix (W m^{-1} K^{-1})	TC of composites (W m^{-1} K^{-1})	Graphene content (wt%)	TCE per 1 wt% graphene loading	Year	Ref.
Randomly dispersed graphene						
Epoxy	0.2	5.8	20	140	2008	S1
Epoxy	0.2	5.1	≈ 15	163	2012	S2
Epoxy	0.22	≈ 11	≈ 59.5	82	2018	S3
Epoxy	0.28	11.2	≈ 32	122	2020	S4
Highly orientation architectures stacked by exfoliated graphene						
Epoxy	0.16	2.13	≈ 1.5	821	2016	S5
PDMS	0.17	2.19	4.8	248	2018	S6
Epoxy	0.21	35.5	33	509	2018	S7
Epoxy	0.23	2.69	≈ 1.6	668	2019	S8
Twisted skeletons formed by continuous CVD graphene nanosheets						
PDMS	0.18	28.77	11.6	1369	2017	S9
Epoxy	0.2	8.8	8.3	518	2018	S10
Natural rubber	0.13	10.64	≈ 13.9	582	2019	S11
PDMS	≈ 0.19	28.12	12	1225	2019	S12
Our work						
PVDF	0.19	12.8	4	1659	This work	

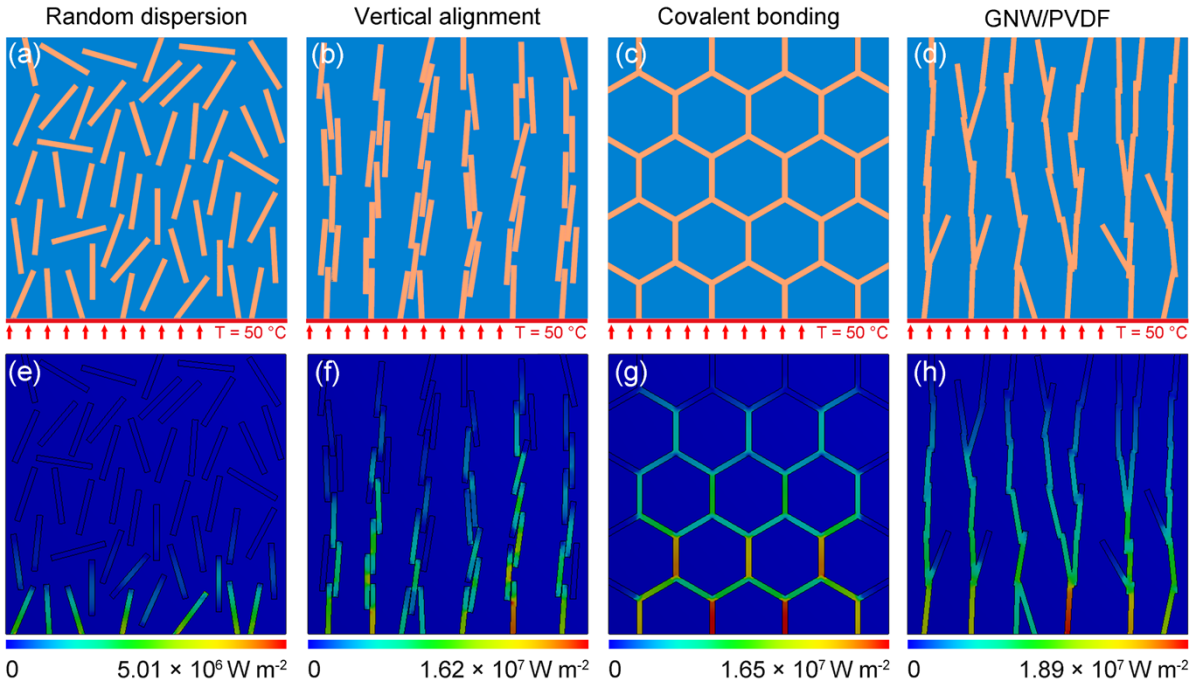

Fig. S3 (a–d) The built models of PVDF matrix embedded with different types of graphene architectures, and (e–h) the corresponding simulated transient heat flux profiles at 0.05 s.

The simulated models were built based on inherent characteristics of various graphene structures, with the same computational domain of 1 mm × 1 mm × 0.05 mm and similar filler volume fractions, as displayed in Figure S3a–d. The yellow part in the models is represented the graphene sheets and the blue background is the PVDF matrix, with the thermal conductivities of 680 W m^{-1} K^{-1} and 0.19 W m^{-1} K^{-1}, respectively [S13]. In a typical simulation process, the initial temperature of all models as well as the ambient temperature were specified to 22 °C, and a constant heat source (50 °C) was set at the bottom of model boxes. The convection coefficient of all exposed surfaces was set as 10 W m^{-2} K^{-1}.

Fig. S3e–h are the heat flux distributions of different models embedded with various graphene frameworks at 0.05 s, in which the heat flow is mainly transferred along the graphene skeletons, and the maximal heat flux of GNW modules is significantly superior than that of other counterparts, indicating that the vertically aligned GNW with covalently bonded interfaces own the best capacity in achieving a fast thermal response rate.

References

S1 S. Ganguli, A. K. Roy and D. P. Anderson, *Carbon*, 2008, **46**, 806-817.

S2 K. M. F. Shahil and A. A. Balandin, *Nano Lett.*, 2012, **12**, 861-867.

S3 F. Kargar, Z. Barani, R. Salgado, B. Debnath, J. S. Lewis, E. Aytan, R. K. Lake and A. A. Balandin, *ACS Appl. Mater. Interfaces*, 2018, **10**, 37555-37565.

S4 Z. Barani, F. Kargar, A. Mohammadzadeh, S. Naghibi, C. Lo, B. Rivera and A. A. Balandin, *Adv. Electron. Mater.*, 2020, **6**, 2000520.

S5 G. Lian, C. C. Tuan, L. Li, S. Jiao, Q. Wang, K. S. Moon, D. Cui and C. P. Wong, *Chem. Mater.*, 2016, **28**, 6096-6104.

S6 M. Qin, Y. Xu, R. Cao, W. Feng and L. Chen, *Adv. Funct. Mater.*, 2018, **28**, 1805053.

S7 F. An, X. Li, P. Min, P. Liu, Z. G. Jiang and Z. Z. Yu, *ACS Appl. Mater. Interfaces*, 2018, **10**, 17383-17392.

S8 Y. Li, W. Wei, Y. Wang, N. Kadhim, Y. Mei and Z. Zhou, *J. Mater. Chem. C*, 2019, **7**, 11783-11789.

S9 H. Fang, Y. Zhao, Y. Zhang, Y. Ren and S.-L. Bai, *ACS Appl. Mater. Interfaces*, 2017, **9**, 26447-26459.

S10 X. Shen, Z. Wang, Y. Wu, X. Liu, Y. B. He, Q. Zheng, Q. H. Yang, F. Kang and J. K. Kim, *Mater. Horiz.*, 2018, **5**, 275-284.

S11 Z. Wu, C. Xu, C. Ma, Z. Liu, H. M. Cheng and W. Ren, *Adv. Mater.*, 2019, **31**, 1900199.

S12 H. Fang, H. Guo, Y. Hu, Y. Ren, P. C. Hsu and S. L. Bai, *Compos. Sci. Technol*, 2020, **188**, 107975.

S13 H. Ci, H. Chang, R. Wang, T. Wei, Y. Wang, Z. Chen, Y. Sun, Z. Dou, Z. Liu, J. Li, P. Gao and Z. Liu, *Adv. Mater.*, 2019, **31**, 1901624.